Synthesis and Crystal Structure of Peptide-2,2′-Biphenyl Hybrids[1])

by **Enrique Mann**[a]), **Ana Montero**[a]), **Miguel A. Maestro**[b]), and **Bernardo Herradón***[a])

[a]) Instituto de Química Orgánica General, C.S.I.C., Juan de la Cierva 3, E-28006 Madrid (e-mail: herradon@iqog.csic.es)

[b]) Servicios Xerais de Apoio á Investigación, Campus da Zapateira s/n, Universidade da Coruña, E-15071 A Coruña

Dedicated to Professor *Dieter Seebach* on the occasion of his 65th birthday

1,1′-Biphenyl derivatives with amino acid/peptide substitution at C(2) and C(2′) (‘*peptide-biphenyl hybrids*’, **6**–**8**) have been prepared by direct *N*-acylation of amino acid/peptide derivatives with 1,1′-biphenyl-2,2′-dicarbonyl dichloride (**5**). Both conformers, which arise from the rotation around the aryl–aryl bond, have been detected by ^{1}H-NMR spectroscopy. Single atropisomers of each **6** ((*R*)-configuration at the stereogenic axis) and **7** ((*S*)-configuration at the stereogenic axis) have been obtained in quantitative yield by slow evaporation of methanolic solutions. The procedures are dynamic atropselective resolutions (*asymmetric transformations of the second kind*). The crystal structures of the peptide-biphenyl hybrids **6** and **7** show highly ordered molecular and supramolecular structures with extensive intramolecular and intermolecular H-bonding.

Introduction. – In connection with a project on the application of the *Heck* reaction to the synthesis of chiral heterocycles, we have recently reported the unexpected formation of compounds **1** and **2** (‘*peptide-biphenyl hybrids*’) from the *o*-iodobenzamides **3** and **4**, respectively, under the *Heck–Overman* conditions (*Scheme 1*) [1]. This is the first report on acyclic compounds that have amino acid or peptide substitution at C(2) and C(2′) of 1,1′-biphenyl[2]). Since both biphenyl derivatives and peptides possess useful properties, the combination of the two functionalities can provide interesting compounds.

Scheme 1

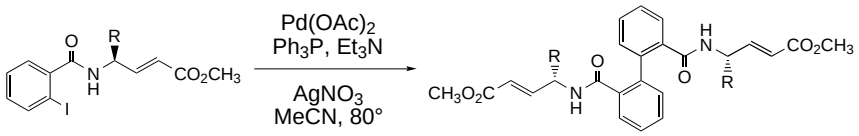

3 R = Me
4 R = i-Pr

1 R = Me
2 R = i-Pr

Peptides are the focus of intense research activity. Although most of the work is motivated by their biological activities [3], they are also useful tools for the study of

[1]) Taken in part from the Ph.D. thesis of *E. M.* (Universidad Autónoma, Madrid, 2002) and the projected Ph.D. thesis of *A. M.*

[2]) The substituents on the 1,1′-biphenyls **1** and **2** are derivatives of γ-amino-α–β-unsaturated acid (vinilogous amino acids), which have been considered as dipeptide mimetics, see [2].

biochemical processes (including protein folding [4]), chiral catalysts for organic synthesis [5], and technological materials [6]. On the other hand, the biphenyl derivatives are present in numerous pharmaceuticals [7]; furthermore, they are extensively used as chiral ligands for asymmetric synthesis [8] as well as mesogenic materials [9].

To deepen our knowledge of peptide-biphenyl hybrids, we have planned to synthesize biphenyl derivatives with saturated peptide chains at C(2) and C(2′) (**A**; *Scheme 2*). Besides the potential practical applications indicated above, we have been attracted by the structural features of this kind of compounds[3]), especially on the mutual influence of both kinds of structural fragments. As a result of the free rotation around the aryl–aryl bond, both peptide chains might interact through intramolecular H-bonds, to give structures of type **A**′. This potential interaction might influence the conformation around the aryl–aryl bond, both the thermodynamic stability of any rotamer (atropisomer) as well as the kinetics of their interconversion. If structure **A**′ is obtained, the biphenyl scaffold will cause a change in the propagation sense of the peptide chains and, in a formal sense, it mimics a β-turn[4]).

Scheme 2

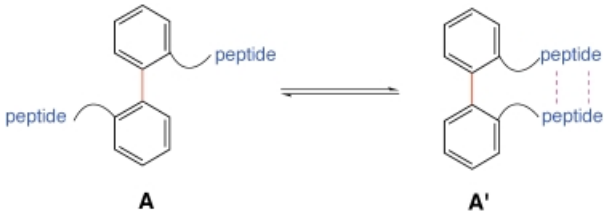

In this paper, we report the straightforward synthesis of peptide-biphenyl hybrids with 1–3 amino acid residues at each phenyl ring, as well as crystallographic studies on some of these compounds.

Results and Discussion. – *Synthesis of Peptide-Biphenyl Hybrids and Preliminary ^{1}H-NMR Study.* The target molecules **6**–**8** have been prepared by direct acylation of *N*-protected amino acid/peptide with 1,1′-biphenyl-2,2′-dicarbonyl dichloride (**5**) [13] in 58–70% isolated yields (*Scheme 3*)[5]). The method is operationally simple and scalable, employing readily available starting materials and reagents. Only a small amount (5–15%) of the corresponding peptidyl fluorenone **B** is obtained as side product.

---

[3]) *Feigel* and co-workers have reported macrocyclic compounds with peptide chains at C(2) and C(2′) of 1,1′-biphenyl [10] as well as conjugates of (a*S*)-2,2′-dimethyl-1,1′-biphenyl-6,6′-dicarboxylic acid with (*S*)- and (*R*)-valine [11], but the structures of these compounds are mainly influenced by particular features: macrocyclic system and 2,2′,6,6′-tetrasubstituted 1,1′-biphenyl.

[4]) It must be mentioned that the biphenyl scaffold does not imitate any particular β-turn, and the similarity is only functional. For a discussion of turns, see [12].

[5]) Since our main motivation was structural, we have not attempted to optimize the synthesis.

Scheme 3

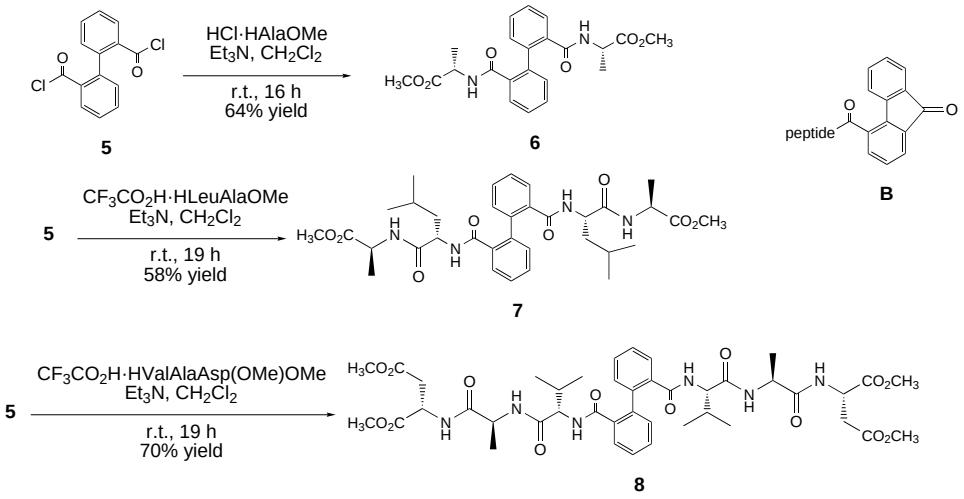

We have observed two set of signals (in nearly 1:1 ratio) in the ^{1}H-NMR spectra of the peptide-biphenyl hybrids **6**–**8**, indicating a slow (in the NMR time-scale) equilibrium between two isomers[6]). Furthermore, there is high dispersion in the chemical shifts of the amide protons (see *Fig. 1* for a representative example), which denotes that the amide protons of the species in solution sample different environments[7]).

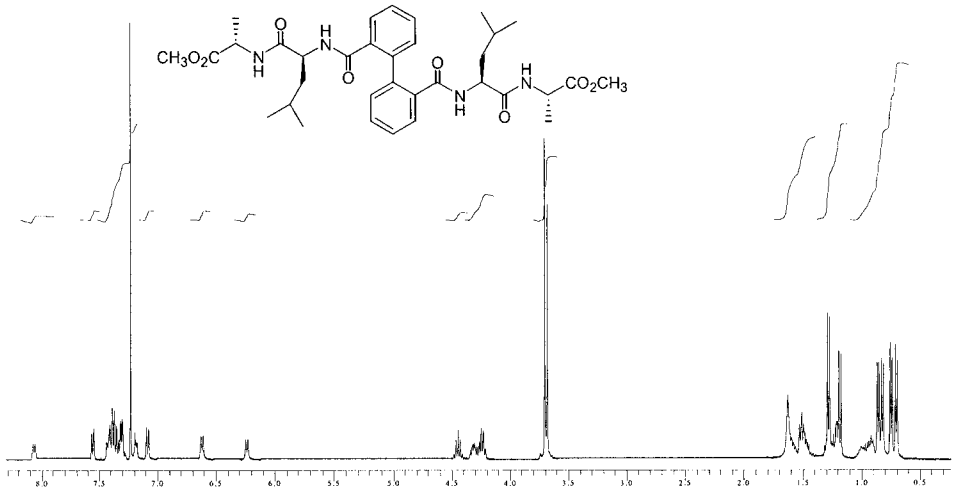

Fig. 1. *^{1}H-NMR Spectrum* (300 MHz, $CDCl_3$, 303 K, 10^{-2} M) *of peptide-biphenyl hybrid* **7**

[6]) Because of the C_2 symmetry, the two chains in the peptide-biphenyl hybrids are chemically equivalent.

[7]) As expected, the ^{1}H-NMR spectra are dependent on the temperature and the solvent. Variable-temperature dynamic ^{1}H-NMR spectroscopy studies are underway.

In principle, although the two equilibrating species can be due to different rotations around the peptide bonds or different conformations of the individual peptide chains, the most likely explanation is the presence of the two rotamers resulting from rotation around the aryl–aryl bond (atropisomers; *Scheme 4*). Since all of the amide bonds in **6**–**8** are secondary, a 1:1 ratio of two amide rotamers is unlikely [14]. On the other hand, the existence of slowly interconverting conformers in the peptide chain is very unlikely on basis of the relatively high mobility of derivatives of short peptides [15]. This suggestion has been corroborated by conformational studies on model compounds such as the peptidyl fluorenones of type **B** and *N*-arylcarbonyl derivatives of amino acids and peptides [16].

Scheme 4

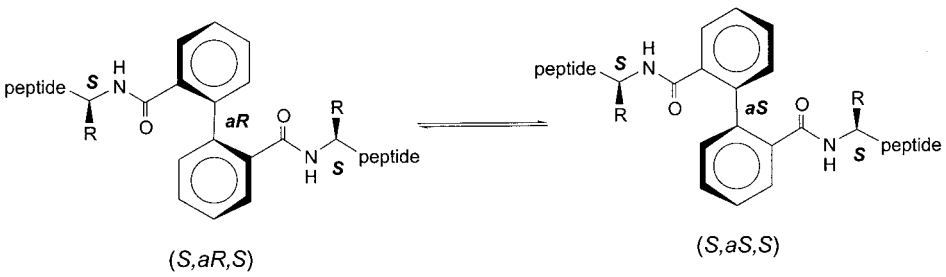

Generally, biaryl derivatives require at least three substituents at the *ortho*-positions to prevent free rotation around the aryl–aryl bond [17]; although, in some special cases, the two rotamers of *ortho*-disubstituted biaryls have been detected by ^{1}H-NMR [18]. Compounds **6**–**8** bear only two substituents at C(2) and C(2′), but each of them contains one to three stereogenic centers as well as functionalities capable of forming H-bonds.

The slow interconversion of the two rotamers ((a*S*) and (a*R*)) (*Scheme 4*) is the consequence of a process with (relatively) high activation energy (the difference between the ground and the transition states). A plausible explanation is that the ground-state is quite stable, and this stability can be due to the presence of strong H-bonds; that is supported by the low-field resonance for most amide protons of **6**–**8**. Further evidence is provided by crystallographic studies on **6** and **7**.

Crystal Structure of the Peptide-Biphenyl Hybrid **6**. Suitable single crystals were obtained by slow evaporation at room temperature of a methanolic solution of **6**, and they have been analyzed by X-ray diffraction[8]). The molecular structure is depicted in *Fig. 2*, and the crystal packing is shown in *Fig. 3*. All molecules in the unit cell have the same sense of the chirality at the stereogenic aryl–aryl bond. Since the configurations of all the amino acid residues are (*S*), we can confidently conclude that the configuration at the stereogenic axis is (a*R*). Since the yield of the crystallization is

[8]) The Me group C(11) of **6** is disordered. The conformation depicted in *Fig. 1* for the O(2)–C(11) bond is the most likely one on the basis of chemical studies.

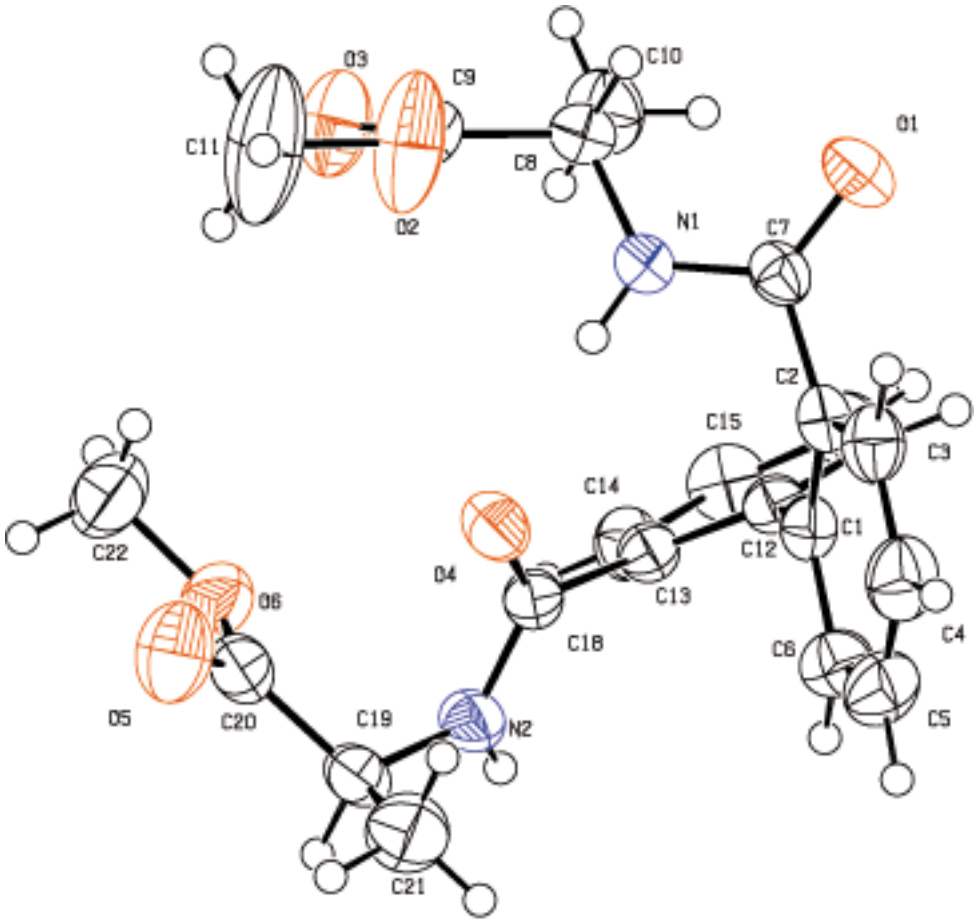

Fig. 2. *ORTEP Plot of the molecular structure of the peptide-biphenyl hybrid* **6**. The thermal ellipsoids are drawn at 50% probability.

nearly quantitative[9]), the transformation is a dynamic atropselective resolution. The shift of the equilibrium is controlled by the (more) efficient crystal packing of the molecules of one of the isomers[10]).

A selection of crystal-structure data of **6** is collected in *Table 1*. The molecular structure of (a*R*)-**6** (*Fig. 2*) displays a dihedral angle of *ca.* 70° between both aromatic

---

[9]) Actually, the single crystals of **6** and **7** were obtained by evaporation almost to dryness; the mass balances of both crystallizations were over 95%. The procedures were reproducible.

[10]) The crystallizations of **6** and **7** have been termed *asymmetric transformations of the second kind* or *crystallization-induced asymmetric transformation* [17].

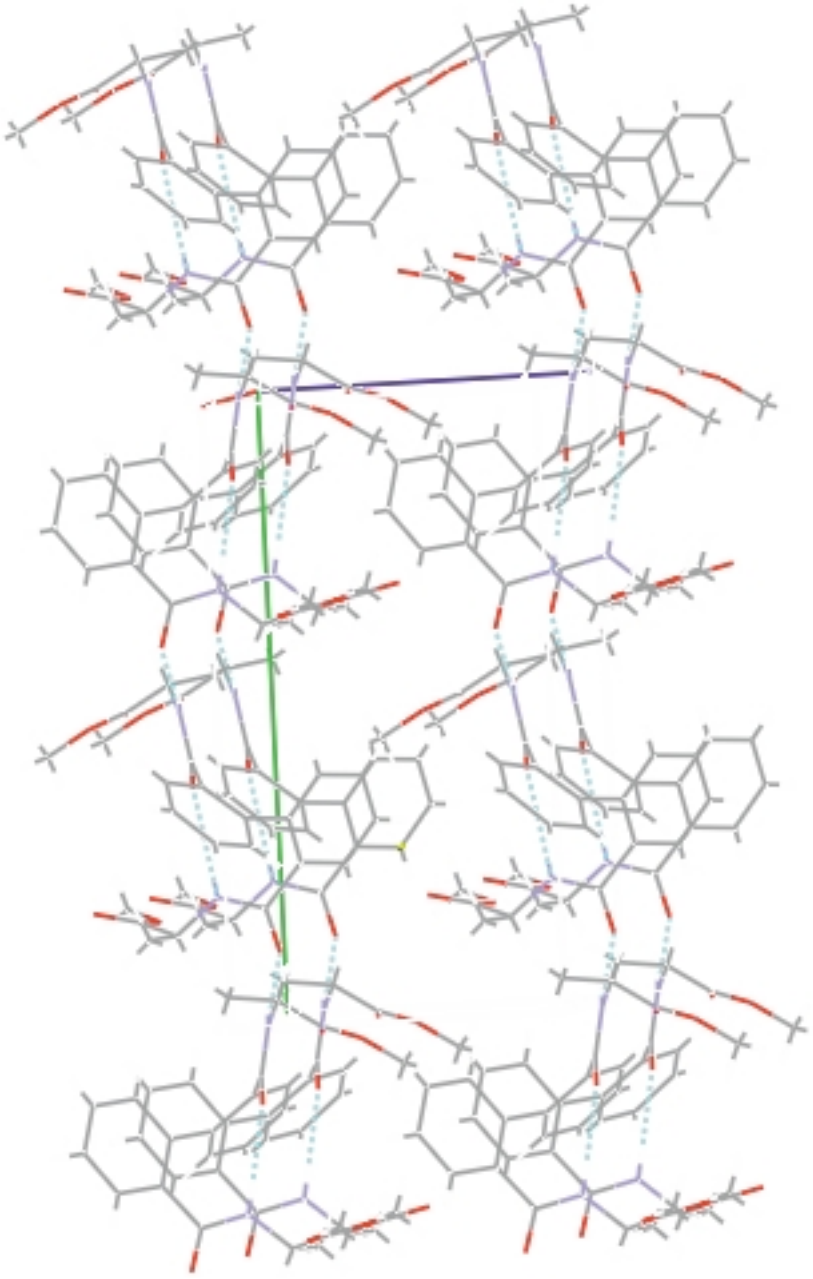

Fig. 3. *Crystal packing and unit-cell representation of the peptide-biphenyl hybrid* **6**, *showing the H-bond pattern*

Table 1. *Selected Structural Parameters for Peptide-Biphenyl Hybrid* **6**[a])

D–H···A[b])	*d*(D–H)	*d*(H···A)	*d*(D···A)	<(DHA)	Class
N(1)–H(1)···O(4)	0.86	2.07	2.912(3)	164.4	Intramolecular
N(2)–H(2)···O(1)[c])	0.86	1.99	2.836(3)	165.7	Intermolecular

Torsion angle	Type	Angle[b])
C(7)–N(1)–C(8)–C(9)	ϕ	−151.3(2)
C(18)–N(2)–C(19)–C(20)	ϕ	53.0(3)
N(1)–C(8)–C(9)–O(3)	φ	59.5(8)
N(2)–C(19)–C(20)–O(6)	φ	41.1(3)
C(2)–C(7)–N(1)–C(8)	ω	176.7(2)
C(13)–C(18)–N(2)–C(19)	ω	178.6(2)
C(1)–C(2)–C(7)–O(1)	phenyl/carbonyl	−125.2(3)
C(12)–C(13)–C(18)–O(4)	phenyl/carbonyl	49.6(4)
C(2)–C(1)–C(12)–C(13)	phenyl/phenyl	−115.8(3)
C(2)–C(1)–C(12)–C(17)	phenyl/phenyl	68.1(3)

[a]) The distances are in Å, and the angles in °. [b]) Standard uncertainties, except for fixing and riding H-atoms are included. [c]) Symmetry transformations used to generate equivalent atoms: $-x, y-1/2, -z$.

rings. An interesting feature is the non-coplanarity between each phenyl ring and its vicinal C=O groups (49–55° deviation from planarity). The torsion angles ϕ are −151.3° and +53.0° for the amino acid residues, which are typical for peptides; thus, the biphenyl unit does not cause any constraint to the residues bonded. Finally, the presence of an intramolecular H-bond between N(1) and O(4) is manifested by the N(1)···O(4) distance of *ca.* 2.91 Å and a N(1)–H(1)–O(4) angle of *ca.* 164°.

An important structural aspect of peptide compounds is their capacity to self-associate, both in solution as well as in the solid state, mediated by intermolecular H-bonds [19]. This characteristic can be useful to understand the interaction with a biomacromolecular target (either an enzyme or a receptor), as well as the properties of peptide-based materials.

An interesting feature of the crystal packing of **6** (*Fig. 3*) is the intermolecular H-bond formed by the NH and CO groups (N(2) and O(1)) that do not participate in the intramolecular interactions. In the crystal packing, each molecule interacts with two neighbors through N–H···O bonds (d(N···O) = 2.84 Å, angle (NHO) = 166°), generating a supramolecular left-handed helix ((*M*)-configuration) (*Fig. 4,a*).

According to the graph-set analysis of H-bonded crystal structures [20], we can classify the intramolecular H-bond as a S(9) motif for each molecule in the asymmetric unit. On the other hand, each intermolecular H-bond is classified as a D motif, resulting in a first-level graph set N_1 = S(9)DD, with a binary graph set $N_2 = C_2^2(9)$.

Thus, the crystals of (a*R*)-**6** presents three levels of chirality: the C(α)-atoms of the amino acid residues ((*S*)-configuration), the axis of the biphenyl system ((a*R*)-configuration), and the supramolecular helix ((*M*)-configuration; *Fig. 4,b*).

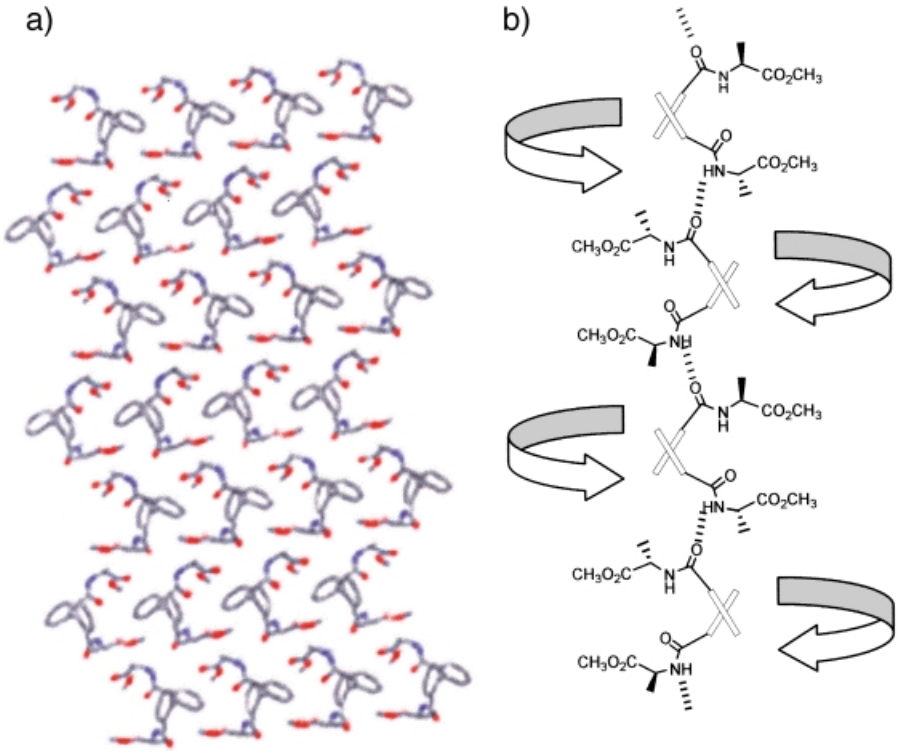

Fig. 4. a) *Crystal packing of* **6**. b) *Schematic representation of the helical supramolecular structure of* **6**.

Crystal Structure of Peptide-Biphenyl Hybrid **7**. Similarly to **6**, single crystals of **7** were obtained by slow evaporation at room temperature of a methanolic solution[9])[10]). The molecular structure and crystal packing are depicted in *Figs. 5* and *6*, respectively. Although the crystallization process and the crystal structure of **7** are quite similar to those of **6**, there are two important differences: the sense of the chirality of the aryl–aryl bond in crystalline **7** is (a*S*)[11]), and the molecules of **7** participate in more H-bonds than those of **6**[12]). The latter results from the higher number of amino acid residues in **7**. The former finding must be a consequence of the subtle structural factors involved in the crystal packing of organic molecules, a phenomenon that has profound implications in the field of crystal engineering [21] and in the study of polymorphs [22].

A selection of structural parameters for compound (a*S*)-**7** is indicated in *Table 2*. As in **6**, the dihedral angle between both aryl rings of **7** is *ca.* 70°, and there is significant deviation from planarity between the phenyl rings and the adjacent C=O group (61° and 64° for each chain). It is remarkable that all of the ϕ and φ angles of the peptide chains lay in the region of extended (β-sheet) conformation in a *Ramachandran* plot

---

[11]) The (a*S*)-configuration at the stereogenic axis has been assigned on the basis of the (*S*)-configuration of the amino acid residues.

[12]) The different packing of **6** and **7** is also manifested in the crystal system (and the space group) as well as in the number of molecules in the asymmetric unit (see *Table 3*).

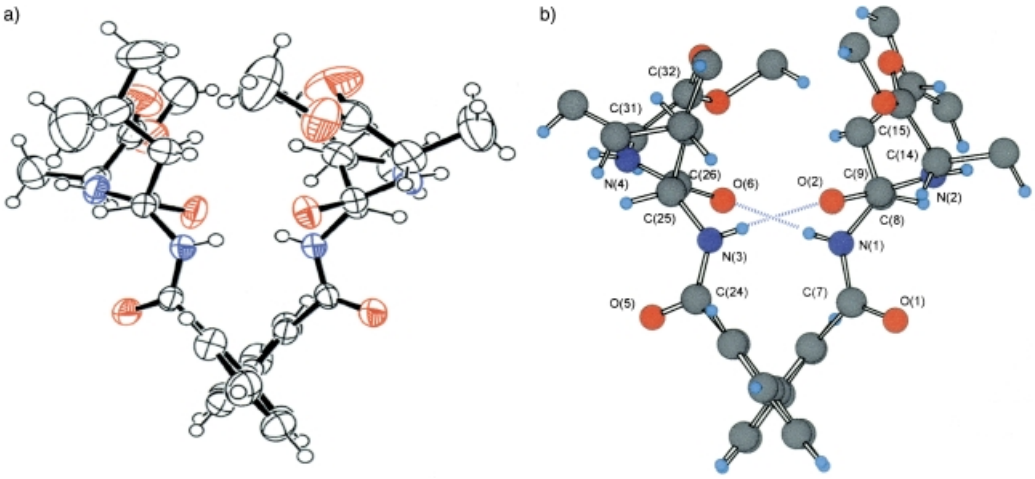

Fig. 5. a) *ORTEP Plot of the molecular structure of the peptide-biphenyl hybrid* **7**. The thermal ellipsoids are drawn at 50% probability. b) *Molecular structure of* **7**, *showing the intramolecular H-bonds.*

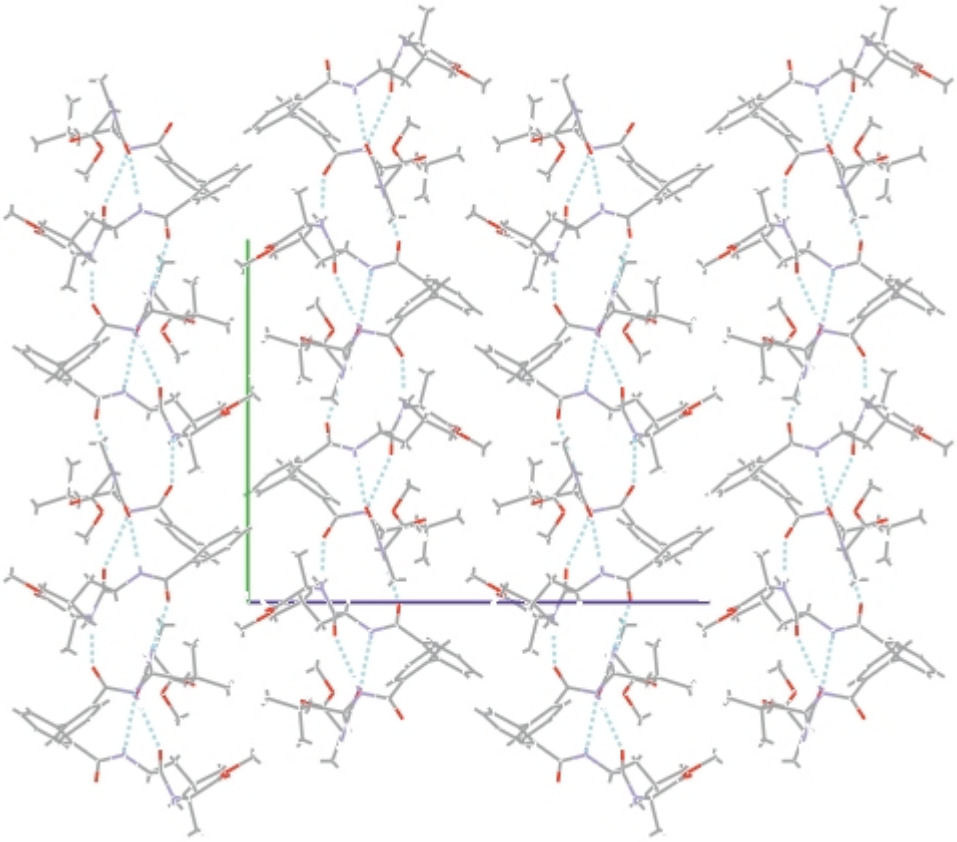

Fig. 6. *Crystal packing of the peptide-biphenyl hybrid* **7**, *showing the H-bond pattern* (view along axis *a*)

Table 2. *Selected Structural Parameters for Peptide-Biphenyl Hybrid* **7**[a])

D–H···A	d(D–H)	d(H···A)	d(D···A)	<(DHA)	Class
N(1)–H(1)···O(6)	0.80(2)	2.07(2)	2.867(2)	169.5(2)	Intramolecular
N(3)–H(3)···O(2)	0.80(2)	2.13(2)	2.927(2)	171(2)	Intramolecular
N(2)–H(2)···O(5)[b])	0.90(2)	2.01(2)	2.913(2)	179(2)	Intermolecular
N(4)–H(4)···O(1)[c])	0.89(3)	2.08(3)	2.966(2)	173(2)	Intermolecular

Torsion angle	Type	Angle
C(7)–N(1)–C(8)–C(9)	ϕ	– 64.5(2)
C(9)–N(2)–C(14)–C(15)	ϕ	– 67.1(3)
C(24)–N(3)–C(25)–C(26)	ϕ	– 73.1(2)
C(26)–N(4)–C(31)–C(32)	ϕ	– 53.6(3)
N(1)–C(8)–C(9)–N(2)	φ	146.11(17)
N(2)–C(14)–C(15)–O(4)	φ	156.70(19)
N(3)–C(25)–C(26)–N(4)	φ	156.20(17)
N(4)–C(31)–C(32)–O(8)	φ	141.4(2)
C(1)–C(7)–N(1)–C(8)	ω	173.62(16)
C(8)–C(9)–N(2)–C(14)	ω	– 170.35(19)
C(19)–C(24)–N(3)–C(25)	ω	171.92(17)
C(25)–C(26)–N(4)–C(31)	ω	– 165.2(2)
C(6)–C(1)–C(7)–O(1)	phenyl/carbonyl	61.2(2)
C(18)–C(19)–C(24)–O(5)	phenyl/carbonyl	64.2(2)
C(1)–C(6)–C(18)–C(19)	phenyl/phenyl	72.1(2)
C(1)–C(6)–C(18)–C(23)	phenyl/phenyl	– 107.8(2)

[a]) The distances are in Å, and the angles in °. Standard uncertainties are included. [b]) Symmetry transformations: $-x+1, y+1/2, -z+1/2$. [c]) Symmetry transformations: $-x+1, y-1/2, -z+1/2$.

[23][13]). Finally, the molecular structure of (a*S*)-**7** presents two intramolecular H-bonds formed by the NH and CO groups of the leucine residue in each chain (see *Fig. 5*,*b*, and *Table 2* for details).

Crystalline (a*S*)-**7** has a highly ordered supramolecular structure (*Fig. 6*), where the NH and CO groups not involved in the intramolecular H-bonds participate in intermolecular bonding (*Table 2*). Thus, any molecule of (a*S*)-**7** interacts with two vicinal molecules, forming an extensive pattern of H-bonds: each amide groups of (a*S*)-**7** participate in two H-bonds, and each molecule of (a*S*)-**7** is involved in six H-bonds. The overall supramolecular arrangement in the crystal displays parallel right-handed helices with (*P*)-configuration (*Fig. 7*).

The H-bond pattern of (a*S*)-**7** can be analyzed as $N_1 = S(12)S(12)DD$ at the first-level graph set, with three binary graph sets, one of them with $N_2 = R_2^2(14)$ and two of them with $N_2 = C_2^2(12)$ [20], also constituting a difference with the crystal structure of (a*R*)-**6** (see above).

Conclusions. – Novel peptide compounds ('*peptide-biphenyl hybrids*') are reported. Although the 1,1′-biphenyl bears only two substituents in *o*- and *o*′-positions, both

[13]) The only slight deviation from the standard geometry of peptide conformations is the dihedral angle around the peptide bond of the terminal residue in one of the chains (– 165°, *Table 2*).

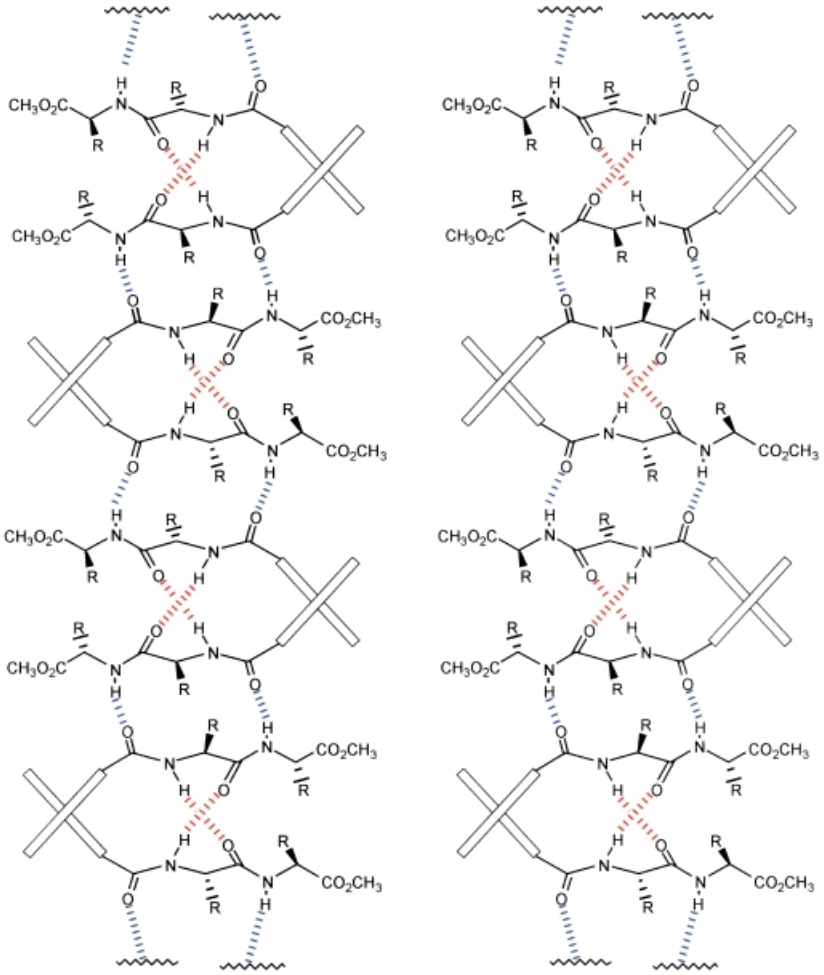

Fig. 7. *Schematic representation of the helical supramolecular structure of two parallel chains of* **7**

rotamers are detected by ^{1}H-NMR, suggesting a (relatively) high-activation-energy process [24]. A reason for the slow interconversion between atropisomers can be that the conformer(s) are very stable due to favorable H-bonding. This hypothesis is corroborated by single-crystal X-ray-diffraction analysis of the peptide-biphenyl hybrids **6** and **7**, which were obtained in a dynamic atropselective resolution. The crystals of **6** and **7** present highly ordered arrangements, where all the peptide bonds participate in H-bonding, resulting in helical supramolecular structures.

Although preliminary, the results reported in the present paper (especially the structure of **7**) indicate that the peptide-biphenyl hybrids resemble a β-turn, a secondary conformational motif with high relevance for the biological activity of peptide [12]. Additionally, we intend to combine the mesogenic features of biphenyl

derivatives [9a] with the highly organized crystal structures of the peptide-biphenyl hybrids to prepare polymers with liquid-crystal behavior[14]).

Financial support from the Spanish Ministry of Science and Technology (Project BQU2001-2270) and *Comunidad Autónoma de Madrid* (Project 08.5/0056/2000-2) is gratefully acknowledged.

Experimental Part

General. All reactions were carried out with dry solvents under Ar. For all prep. chromatographic purifications, silica gel (40–63 nm) was used. The melting points were measured on a *Kofler* hot-stage apparatus and are uncorrected. The optical rotations were determined with a *Perkin-Elmer 241 MC* polarimeter at r.t. (*ca.* 295 K). The IR spectra were measured in CH_2Cl_2 solution in a *Perkin-Elmer 657* spectrometer; the frequencies in the IR spectra are indicated in cm^{-1}. ^1H- and ^{13}C-NMR spectra were measured with *Varian INOVA 400* and *Varian INOVA 300*; chemical shifts (δ) are reported in ppm, and the coupling constants (J) are indicated in Hz. ^1H-NMR Spectra were referenced to the chemical shift of either TMS (δ 0.00 ppm) or the residual proton in the deuterated solvent. ^{13}C-NMR Spectra were referenced to the chemical shift of the deuterated solvent. The multiplicity of the signals in the ^{13}C-NMR spectra was determined by APT, DEPT, or HMQC experiments. Electrospray mass spectra (ES-MS) were recorded with a *Hewlett-Packard MDS-1100* equipment. Electron-impact mass spectra (EI-MS) were measured with a *Hitachi-Perkin-Elmer RMU-GMG* spectrometer. The units in the mass spectra are in m/z. Combustion analysis were realized in a *Carlo Erba EA 1180-Elemental Analyzer. Kofler* hot-stage apparatus and are uncorrected. All the preparative chromatographies were done on silica gel (40–63 nm).

Dimethyl N,N′*-[(a*R*)-1,1′-biphenyl-2,2′-dicarbonyl]bis[(*S*)-alaninate]* (**6**). Et_3N (4.44 ml, 32.25 mmol) and (*S*)-H-Ala-OMe · HCl (3.18 g, 22.58 mmol) were added to a soln. of **5** (3.0 g, 10.75 mmol) in CH_2Cl_2 (50 ml). The mixture was stirred at r.t. for 16 h, and taken up with H_2O. The phases were separated, and the aq. one was extracted with CH_2Cl_2 (2 × 50 ml). The combined org. extracts were dried ($MgSO_4$). The org. solvent was removed under vacuum to give a crude product, which was purified by chromatography (hexane/AcOEt 4 : 1 to 2 : 3) to give **6** (2.85 g, 64% yield). M.p. 132–134°. $[\alpha]_D = -53$ ($c = 0.5$, MeOH). IR: 3430, 3264, 1745, 1737, 1656, 1632, 1550, 1454, 1335, 1214, 1170, 1111, 763. ^1H-NMR (400 MHz, $CDCl_3$, 303 K, mixture of rotamers): 7.58 (*m*, 2 arom. H); 7.49 (*d*, $J = 7.6$, 0.8 H, NH); 7.39 (*m*, 4 arom. H); 7.33 (*m*, 1.2 H, NH); 7.17 (*m*, 2 arom. H); 4.53 (*m*, 2 H, α-CH); 3.69 (*s*, 3.6 H, CO_2Me); 3.60 (*s*, 2.4 H, CO_2Me); 1.28 (*d*, $J = 7.1$, 2.4 H, Me); 1.09 (*d*, $J = 7.2$, 3.6 H, Me). ^{13}C-NMR (75 MHz, $CDCl_3$, 303 K, mixture of conformers): 173.5 (*s*); 173.2 (*s*); 169.6 (*s*); 169.5 (*s*); 139.3 (*s*); 138.9 (*s*); 135.9 (*s*); 135.8 (*s*); 130.1 (*d*); 130.0 (*d*); 129.9 (*d*); 129.7 (*d*); 128.1 (*d*); 127.9 (*d*); 127.4 (*d*); 127.3 (*d*); 52.6 (*q*); 48.4 (*d*); 48.2 (*d*); 18.2 (*q*); 17.8 (*q*). EI-MS: 412 (1, M^+), 353 (13), 310 (46), 282 (100), 250 (17), 222 (38), 181 (93), 152 (36) 104 (20). Anal. calc. for $C_{22}H_{24}N_2O_6$: C 64.07, H 5.87, N 6.79; found: C 64.20, H 5.80, N 6.76.

Dimethyl N,N′*-[(a*S*)-1,1′-Biphenyl-2,2′-dicarbonyl]bis[(*S*)-leucyl-(*S*)-alaninate]* (**7**). Et_3N (1.04 ml, 7.56 mmol) and (*S,S*)-H-Leu-Ala-OMe trifluoroacetate (1.04 g, 3.16 mmol) were added to a soln. of **5** (352 mg, 1.26 mmol) in CH_2Cl_2 (10 ml). The mixture was stirred at r.t. for 19 h; and treated with H_2O. The phases were separated, and the aq. one was extracted with CH_2Cl_2 (2 × 10 ml). The combined org. extracts were dried ($MgSO_4$). The org. solvent was removed under vacuum to give a crude product, which was purified by chromatography (hexane/AcOEt 2 : 3) to give **7** (466 mg, 58% yield). M.p. 209–215°[15]). $[\alpha]_D = -88$ ($c = 0.5$, MeOH). IR: 3430, 3260, 1754, 1638, 1547. ^1H-NMR (300 MHz, $CDCl_3$, 303 K, mixture of rotamers): 7.99 (*d*, $J =$ 7.8, 1 H, NH-Leu); 7.60 (*m*, 1 arom. H); 7.45 (*m*, 1 arom. H); 7.40–7.35 (*m*, 5 H, 4 arom. H, NH-Leu); 7.23 (*m*, 1 arom. H); 7.14 (*m*, 1 arom. H); 6.62 (*d*, $J = 7.5$, 1 H, NH-Ala); 6.26 (*d*, $J = 7.1$, 1 H, NH-Ala); 4.49 (*m*, 1 H, α-CH-Ala); 4.35 (*m*, 1 H, α-CH-Leu); 4.30 (*m*, 2 H, α-CH-Ala, α-CH-Leu); 3.73 (*s*, CO_2Me); 3.71 (*s*, CO_2Me); 1.55 (*m*, 3 H, Leu-side chain); 1.32 (*d*, $J = 7.2$, 3 H, Me(Ala)); 1.26 (*m*, 2 H, Leu-side chain); 1.22 (*d*, $J = 7.1$, 3 H,

---

14) *a*) We have achieved the polymerization of peptide-biphenyl hybrids with acyclic α,ω-diols to give polyesters, which have aromatic, peptidic, and acyclic fragments (*A. Montero*, *P. Bello*, *B. Herradón*, unpublished results). The structural characterization and assessment of physicochemical properties are in progress. *b*) For a discussion on the influence of aromatic fragments on the conformation of polyesters and model compounds, see [25].

15) The ample interval in the melting of **7** can be due to either the existence of two equilibrating species or to the formation of mesophases.

Me(Ala)); 1.10 (*m*, 1 H, Leu-side chain); 0.90 (*d*, *J* = 6.4, Me); 0.86 (*d*, *J* = 6.4, Me); 0.79 (*d*, *J* = 6.7, Me); 0.75 (*d*, *J* = 6.5, Me). ^{13}C-NMR (75 MHz, $CDCl_3$, 303 K, mixture of conformers): 173.0; 171.8; 171.2; 170.1; 169.8; 139.0; 138.1; 136.4; 135.4; 130.3; 129.9; 128.7; 127.9; 127.5; 126.4; 52.4; 51.9; 48.0; 40.4; 40.2; 24.7; 24.3; 23.0; 22.8; 22.0; 21.6; 18.2; 17.9. ES-MS (positive mode): 639 (100, $[M+H]^+$). Anal. calc. for $C_{34}H_{46}N_4O_8$: C 63.93, H 7.26, N 8.77; found: C 64.25, H 7.14; N 8.90.

Tetramethyl N,N′-(1,1′-Biphenyl-2,2′-dicarbonyl)bis[(S)-valinyl-(S)-alaninyl-(S)-aspartate] (**8**). Et_3N (1.25 ml, 9.07 mmol) and (*S*,*S*,*S*)-H-Val-Ala-Asp(OMe)-OMe trifluoroacetate (1.61 g, 3.62 mmol) were added to a soln. of **5** (422 mg, 1.51 mmol) in CH_2Cl_2 (15 ml). The mixture was stirred at r.t. for 19 h, and treated with H_2O. The phases were separated, and the aq. one was extracted with CH_2Cl_2 (2 × 15 ml). The combined org. extracts were dried ($MgSO_4$). The org. solvent was removed under vacuum to give a crude product, which was purified by chromatography (hexane/AcOEt 2 : 3) to give **8** (917 mg, 70% yield). M.p. 93–94°. $[\alpha]_D = -15$ (*c* = 0.5, $CHCl_3$). IR: 3403, 3060, 2961, 1742, 1641, 1529, 1438, 1371, 1219, 1172. ^{1}H-NMR (400 MHz, $CDCl_3$, 303 K, mixture of rotamers): 7.79 (*d*, *J* = 7.3, 1 H, NH); 7.67 (*m*, 1 H, NH); 7.54 (*m*, 1 H); 7.40 (*m*, 4 H); 7.17 (*m*, 3 H); 7.10 (*d*, *J* = 7.9, 1 H, NH); 7.06 (*d*, *J* = 8.1, 1 H, NH); 6.99 (*d*, *J* = 7.5, 1 H, NH); 6.13 (*d*, *J* = 7.6, 1 H, NH); 4.79 (*m*, 2 H, α-CH); 4.45 (*quint.*, *J* = 7.3, 1 H, α-CH-Ala); 4.37 (distorted *quint.*, *J* = 7.3, 1 H, α-CH-Ala); 4.15 (*dd*, *J* = 8.0, 6.0, 1 H, α-CH); 4.06 (distorted *t*, *J* = 6.9, 1 H, α-CH); 3.70 (*s*, 6 H, CO_2Me); 3.64 (*s*, 4 H, CO_2Me); 3.58 (*s*, 2 H, CO_2CH_3, minor conformer); 2.95 (*m*, 2 H, CH_2CO_2Me); 2.85 (*m*, 1 H, CH_2CO_2Me); 2.76 (*m*, 1 H, CH_2CO_2Me); 2.02 (*m*, 1 H, Me_2CH); 1.28 (*d*, *J* = 7.1, 3 H, Me(Ala)); 1.26 (*d*, *J* = 7.1, 3 H, Me(Ala)); 0.81 (*d*, *J* = 6.8, 6 H, 2 Me(Val)); 0.68 (*d*, *J* = 6.8, 3 H, Me(Val)); 0.61 (*d*, *J* = 6.8, 3 H, Me(Val)). ^{13}C-NMR (75 MHz,

Table 3. *Crystal Data and Structure Refinement for the Peptide-Biphenyl Hybrids* **6** *and* **7**

	6	**7**
Empirical formula	$C_{22}H_{24}N_2O_6$	$C_{34}H_{46}N_4O_8$
Formula weight [g mol^{-1}]	412.43	638.75
Crystal system	Monoclinic	Orthorhombic
Space group	$P2_1$	$P2_12_12_1$
Z	2	4
a [Å]	8.0731(8)	10.2294(4)
b [Å]	16.1719(16)	16.5393(6)
c [Å]	8.8828(9)	21.0920(8)
β [deg]	113.488(2)	90
V [Å^3]	1063.62(18)	3568.5(2)
F(000)	436	1368
D_x [g cm^{-3}]	1.288	1.189
μ_{calc} [mm^{-1}]	0.094	0.085
Transmission factors (max; min)	0.9944; 0.9768	0.9709; 09587
Scan type	*ϕ* and *ω*	*ϕ* and *ω*
Θ Range for data collection [°]	2.50–26.37	1.93–28.32
Total refl. measured	6250	25451
Independent refl. (*R* (int))	3095 [0.0318]	8850 [0.0341]
Completeness to Θ_{max} [%]	99.4%	99.6%
Absorption correction	Semi-empirical	Semi-empirical
Refinement method	Full-matrix least-squares on F^2	Full-matrix least-squares on F^2
Parameters refined, restraints	291, 1	559, 0
Final *R*1 [$I > 2\sigma(I)$][a])	0.0388	0.0467
*WR*2 (all data)[a])	0.0940	0.1139
Weights (*a*)[b])	0.0457	0.0627
Goodness-of-fit on F^2	1.024	0.952
$\Delta\rho$ (max; min) [e Å^{-3}]	0.165; −0.143	0.249 and −0.169

[a]) $R1 = \Sigma|\,|F_o| - |F_c|\,|/\Sigma|F_o|$ and $wR2 = \{\Sigma[w(F_o^2 - F_c^2)^2]/\Sigma[w(F_0^2)^2]\}^{1/2}$. [b]) Weighting scheme, $w = [\sigma^2(F_0{}^2 + aP^2]$ and $P = (|F_0|^2 + 2|F_c|^2)/3$.

(D_6)DMSO, 303 K, mixture of conformers): 172.1; 170.9; 170.3; 169.9; 168.9; 138.8; 136.2; 129.2; 127.2; 57.9; 52.1; 51.6; 48.4; 47.7; 40.8; 40.3; 39.9; 39.5; 39.1; 38.7; 38.2; 35.5; 30.1; 18.9; 18.1; 17.5. ES-MS (positive mode): 891 ($[M+Na]^+$), 869 (100, $[M+H]^+$). Anal. calc. for $C_{42}H_{56}N_6O_{14}$: C 58.05, H 6.50, N 9.67; found: C 57.66, H 6.72, N 9.71.

Crystal-Structure Analysis of **6** *and* **7**[16]). Data collection was carried out at r.t. on a *Bruker SMART-CCD* area diffractometer with graphite monochromated MoK_α radiation ($\lambda = 0.71073$ Å) operating at 50 kV and 30 mA. Suitable single crystals were obtained by slow evaporation at r.t. of MeOH solns. of **6** (block, colorless, $0.25 \times 0.14 \times 0.06$ mm^3) and **7** (block, colorless, $0.50 \times 0.40 \times 0.35$ mm^3). A total of 1271 frames of intensity data were collected over a hemisphere of the reciprocal space by combination of three exposure sets. Each frame covered 0.3° in ω, and the first 50 frames were recollected at the end of data collection to monitor crystal decay. Absorption corrections were applied with the SADABS program [26]. The structure was solved with the *Bruker* SHELXTL-PC software [27] by direct methods on F^2. The H-atoms were included in calculated positions and refined in the riding mode. The details of the data collection and refinement are given in *Table 3*. The structure drawings were prepared with the PLATON [28], ORTEP-3 [29], and MERCURY [30] programs. The absolute configurations at the stereogenic centers and axes were assigned on basis to the synthetic schemes that start from (*S*) amino acids.

REFERENCES

[1] F. Sánchez-Sancho, E. Mann, B. Herradón, *Adv. Synth. Catal*. **2001**, *343*, 360.
[2] M. Hagihara, N. J. Anthony, T. J. Stout, J. Clardy, S. L. Schreiber, *J. Am. Chem. Soc*. **1992**, *114*, 6568.
[3] a) 'Peptides: Synthesis, Structures, and Applications', Ed. B. Gutte, Academic Press, San Diego, 1995; b) A. Giannis, F. Rübsam, *Adv. Drug Res.* **1997**, *29*, 1.
[4] a) R. L. Baldwin, G. D. Rose, *TIBS* **1999**, *24*, 26; b) I. L. Karle, *Acc. Chem. Res.* **1999**, *32*, 693; c) R. B. Hill, D. P. Raleig, A. Lombardi, W. F. DeGrado, *Acc. Chem. Res.* **2000**, *33*, 745.
[5] E. R. Jarvo, G. T. Copeland, N. Papaioannou, P. J. Bonitatebus, S. J. Miller, *J. Am. Chem. Soc*. **1999**, *121*, 11638.
[6] a) N. Voyer, *Top. Curr. Chem.* **1997**, *184*, 1; b) T. J. Deming, *Adv. Mater*. **1997**, *9*, 299.
[7] a) P. J. Hajduk, M. Bures, J. Praestgaard, S. W. Fesik, *J. Med. Chem.* **2000**, *43*, 3443; b) D. J. Suich, S. A. Mousa, G. Singh, G. Liapakis, T. Reisine, W. F. DeGrado, *Bioorg. Med. Chem*. **2000**, *8*, 2229.
[8] M. McCarthy, P. J. Guiry, *Tetrahedron* **2001**, *57*, 3809.
[9] a) C. Lazar, M. D. Wand, R. P. Lemieux, *J. Am. Chem. Soc*. **2000**, *122*, 12586; b) E. R. Zubarev, M. U. Pralle, E. D. Sone, S. I. Stupp, *J. Am. Chem. Soc*. **2001**, *123*, 4105.
[10] a) V. Brandmeier, M. Feigel, *Tetrahedron* **1989**,*45*, 1365; b) V. Brandmeier, M. Feigel, M. Bremer, *Angew. Chem.*, *Int. Ed*. **1989**, *28*, 486; c) V. Brandmeier, W. H. B. Sauer, M. Feigel, *Helv. Chim. Acta* **1994**, *77*, 70.
[11] C. Weigand, M. Feigel, C. Landgrafe, *Chem. Commun*. **1998**, 679.
[12] G. D. Rose, L. M. Gierasch, J. A. Smith, *Adv. Protein Chem*. **1985**, *37*, 1.
[13] a) H. W. Underwood, E. L. Kochmann, *J. Chem. Soc*. **1924**, *46*, 2069; b) J. S. Walia, J. Singh, M. S. Chattha, M. Satyanarayana, *Tetrahedron Lett*. **1969**, 195.
[14] G. Fischer, *Chem. Soc. Rev*. **2000**, *29*, 119.
[15] H. J. Dyson, P. E. Wright, *Annu. Rev. Biophys. Biomol. Struct.* **1991**, *20*, 519.
[16] E. Mann, Master Thesis, Universidad Autónoma, Madrid, Spain, 2000.
[17] E. L. Eliel, S. H. Wilen, 'Stereochemistry of Organic Compounds', John Wiley & Sons, New York, 1994.
[18] Y. Imai, W. Zhang, T. Kida, Y. Nakatsuji, I. Ikeda, *J. Org. Chem*. **2000**, *65*, 3326.
[19] a) G. M. Whitesides, E. E. Simanek, J. P. Mathias, C. T. Seto, D. N. Chin, M. Mammen, D. M. Gordon, *Acc. Chem. Res.* **1995**, *28*, 37; b) D. S. Lawrence, T. Jiang, M. Levett, *Chem. Rev.* **1995**, *95*, 2229; c) D. Ranganathan, S. Kurur, K. P. Madhusudanan, I. L. Karle, *Tetrahedron Lett*. **1997**, *38*, 4659; d) J. S. Nowick, M. Pairish, I. Q. Lee, D. L. Holmes, J. W. Ziller, *J. Am. Chem. Soc*. **1997**, *119*, 5413; e) D. T. Bong, M. R. Ghadiri, *Angew. Chem.*, *Int. Ed*. **2001**, *40*, 2163.
[20] J. Bernstein, R. E. Davis, L. Shimoni, N.-L. Chang, *Angew. Chem.*, *Int. Ed*. **1995**, *34*, 1555.

---

16) Crystallographic data (excluding structure factors) have been deposited with the *Cambridge Crystallographic Data Centre* as deposition numbers CCDC-186485 (**6**) and CCDC-186484 (**7**). Copies of the data can be obtained, free of charge, on application to the CCDC, 12 Union Road, Cambridge CB2 1EZ UK (fax: +44(1223)336033; e-mail: deposit@ccdc.cam.ac.uk).

[21] a) G. R. Desiraju, 'Crystal Engineering. The Design of Organic Solids', Elsevier, Amsterdam, 1989; b) C. B. Aakeröy, K. R. Seddon, *Chem. Soc. Rev.* **1993**, 397; c) G. R. Desiraju, *Angew. Chem.*, *Int. Ed.* **1995**, *34*, 2311; d) T. Steiner, *Angew. Chem.*, *Int. Ed.* **2002**, *41*, 48.
[22] a) A. Gavezzotti, *Chem. Phys. Lett.* **1989**, *161*, 67; b) J. S. Miller, *Adv. Mater.* **1998**, *10*, 1553.
[23] G. N. Ramachandran, V. Sasisekharan, *Adv. Protein Chem.* **1968**, *23*, 283.
[24] M. Ōki, *Topics Stereochem.* **1983**, *14*, 1.
[25] N. J. Heaton, P. Bello, B. Herradón, A. del Campo, J. Jiménez-Barbero, *J. Am. Chem. Soc.* **1998**, *120*, 9632.
[26] G. M. Sheldrick, 'Program for Absortion Corrections Using Bruker CCD Data', University of Göttingen, Germany, 1986.
[27] G. M. Sheldrick, University of Göttingen, Germany, 1996.
[28] a) A. L. Spek, PLATON, 'Program for the Analysis of Molecular Geometry', University of Utrecht, The Netherlands, 2001; b) Web address: http://www.cryst.chem.uu.nl/platon.
[29] a) L. J. Farrugia, *J. Appl. Crystallogr.* **1997**, *30*, 565; b) Web address: http://www.chem.gla.ac.uk/~louis/software/ortep3.
[30] Web address: http://www.ccdc.cam.ac.uk/prods/mercury.

Received May 30, 2002